

Computerized Planning for Multiprobe Cryosurgery using a Force-field Analogy

DAVID C. LUNG^a, THOMAS F. STAHOVICH^b and YOED RABIN^{a,*}

^aDepartment of Mechanical Engineering, Carnegie Mellon University, Pittsburgh, PA 15213, USA;

^bDepartment of Mechanical Engineering, University of California, Riverside, CA 92521, USA

(Received 10 June 2003; In final form 27 February 2004)

Cryosurgery is the destruction of undesired biological tissues by freezing. For internal organs, multiple cryoprobes are inserted into the tissue with the goal of maximizing cryoinjury within a predefined target region, while minimizing cryoinjury to the surrounding tissues. The objective of this study is to develop a computerized planning tool to determine the best locations to insert the cryoprobes, based on bioheat transfer simulations. This tool is general and suitable for all available cooling techniques and hardware. The planning procedure employs a novel iterative optimization technique based on a force-field analogy. In each iteration, a single transient bioheat transfer simulation of the cryoprocure is computed. At the end of the simulation, regions of tissue that would have undesired temperatures apply “forces” to the cryoprobes directly moving them to better locations. This method is more efficient than traditional numerical optimization techniques, because it requires significantly fewer bioheat transfer simulations for each iteration of planning. For demonstration purposes, 2D examples on cross sections typical of prostate cryosurgery are given.

Keywords: Cryosurgery; Computerized planning; Bioheat transfer; Prostate

INTRODUCTION

Cryosurgery, which is the destruction of undesired biological tissues by freezing, has been known as an invasive surgical technique since 1961, when Cooper and Lee invented the first cryoprobe [1]. Cryosurgery as a minimally invasive technique has been known since the mid 1980s, when development of minimally invasive cryodevices took place in both Europe and the United States, simultaneously. The earlier devices were based on 5 [2] or 6 “cryoprobes” (Erbe Elektromedizin GmbH, Germany), which could be operated simultaneously. Due to its superior cooling capabilities, liquid nitrogen boiling was the most common cooling technique for invasive cryosurgery until the 1990s. Then, new developments in Joule–Thomson cooling—the cooling effect associated with a sudden relief of a pressurized gas—led to a dramatic decrease in the size of cryoprobes and an increase in the number of cryoprobes that could be used simultaneously (Endocare, Inc., CA; Galil-Medical, Inc., Israel). For example, modern Joule–Thomson devices can simultaneously operate as many as 14 cryoprobes (Cryoseeds[®], Galil-Medical, Inc., Israel). Although

Joule–Thomson cooling leads to a lower cooling power in each cryoprobe, the overall effect of the increased number of cryoprobes makes Joule–Thomson cooling comparable to liquid nitrogen cooling for clinical applications. If localized effectively, however, one of the primary benefits of using a large number of miniaturized cryoprobes is improved control over the freezing process.

Currently, the process of selecting the correct placement of the cryoprobes for a specific procedure (“cryoprobe localization”) is an art held by the cryosurgeon, based on the his or her experience and rules of thumb. Cryoprobes are typically operated in a trail-and-error fashion, until the entire target volume is thought to be frozen. Currently, there are no means to determine the optimal locations for the cryoprobes. Suboptimal localization may leave regions in the target volume unfrozen, may lead to cryoinjury of healthy surrounding tissues, may require an unnecessarily large number of cryoprobes, may increase the duration of the surgical procedure, and may increase the likelihood of post cryosurgery complications, all of which affect the quality and cost of the medical treatment. Computerized planning tools would help to alleviate these difficulties.

*Corresponding author. Address: 5000 Forbes Avenue, Pittsburgh, PA 15213, USA. Fax: +1-412-268-3348. E-mail: rabin@cmu.edu

The essential task for a planning tool is to identify the best locations for the cryoprobes so as to maximize the amount of the target region that is cryoinjured, while minimizing cryoinjury external to the target region. Thus, planning is an optimization problem. Optimization algorithms typically search for an optimum by iteratively improving an initial solution. Conventional optimization techniques typically require multiple evaluations of the objective function (the function to be optimized) for each iteration. For example, gradient based algorithms would require multiple function evaluations to compute the gradients [3]. Here, the objective function involves computing a bioheat transfer simulation of freezing. Such simulations are computationally expensive, in part because of the phase change that occurs. Because of the large number of computationally expensive bioheat transfer simulations that would be required, conventional optimization techniques are not suitable for cryosurgical planning. Our goal is to produce planning tools that are fast enough that they can be used by the cryosurgeon with the patient in the operating room. Towards this goal, we present a novel optimization technique that requires only one simulation per iteration, and can often solve the problem in just 10–20 iterations. The technique is based on a force-field analogy, in which regions of tissue that would have undesirable temperatures apply forces to the cryoprobes, directly moving them to better locations.

RELATED WORK

Keanini and Rubinsky [4] reported on a numerical optimization technique for prostate cryosurgery planning. In that study, the task was to optimize the number of cryoprobes, their diameter, and their active length. Thus, there were three variables to be optimized. The prostate was modeled as a truncated cone with the urethra as a coaxial cylinder. The locations of the cryoprobes were determined by first dividing the prostate into a number of equiangular subregions equal to the number of cryoprobes. One cryoprobe was placed at the centroid of each such subsection. The resulting configuration was a set of cryoprobes placed at equal intervals along the circumference of a circle. The study employed a 3D transient heat transfer simulation. The quantity they minimized was the ratio of the volume of the frozen extraprostatic tissue to the volume of the prostate, evaluated at the time that the entire prostate becomes frozen. This study assumed symmetry and constant material properties in order to reduce simulation costs. In the current study, we consider asymmetric geometry (offset urethra) and material properties that depend on temperature.

The study in Ref. [4] employed the simplex optimization method, which proved to be well suited to the problem formulation used there. In general, the simplex method is known to work well for problems that are linear, or nearly so [3,5]. In our study, we optimize the location of the cryoprobes. This results in a highly non-linear

problem, for which the simplex method is not likely to be effective. In addition, there are significantly more variables to optimize. Keanini and Rubinsky suggest that if other optimization techniques are used for problems like the one they studied, those methods that compute explicit derivatives are likely to be inefficient. Our work employs a novel technique that avoids calculating derivatives so as to minimize the number of simulations needed for each step of optimization.

Shimada and Gossard [6], and Yamakawa and Shimada [7], have used a force-field approach for constructing meshes for finite element analysis. To mesh a geometric domain, the domain is first filled with a set of bubbles (spheres). Repulsive forces between the bubbles distribute them throughout the domain. The centers of the bubbles are then connected together to form the mesh. Kim [8] has used a force-based method to pack objects into a volume. To begin, the objects are placed at default locations within the volume. The intersections between the objects are calculated, and forces are applied in proportion to the intersection volumes. The forces displace the objects so as to relieve the intersections. The process is applied iteratively. Our task is similar but there are differences. We are trying to achieve complete coverage of the target area, rather than a non-intersecting configuration of objects. Also, we are not packing the target regions with objects of known size—the size of the frozen region around a given cryoprobe depends on the proximity to other cryoelements.

NUMERICAL SIMULATIONS

During planning it is necessary to compute bioheat transfer simulations of the cryoprocure. The numerical simulation scheme used in this study has been presented elsewhere [9], and is presented here briefly. It is customary to assume that heat transfer in the presence of blood perfusion can be modeled by the classical bioheat equation [10]:

$$C \frac{\partial T}{\partial t} = \nabla \cdot (k \nabla T) + \dot{w}_b C_b (T_b - T) + \dot{q}_{\text{met}} \quad (1)$$

where C is the volumetric specific heat of the tissue, T is the temperature, t is the time, k is the thermal conductivity of the tissue, \dot{w}_b is the blood perfusion rate (measured in volumetric blood flow rate per unit volume of tissue), C_b is the volumetric specific heat of the blood, T_b is the blood temperature entering the thermally treated area (typically the normal body temperature), and \dot{q}_{met} is the metabolic heat generation.

The classical bioheat equation is commonly assumed to be suitable for representing heat flow in the presence of a dense capillary network. It is unsuitable if there are major blood vessels. In practice, the blood perfusion rate is often found by regression of experimental data against theoretical predictions, based on the classical bioheat equation [11]. Numerous scientific reports have been

TABLE I Representative thermophysical properties of biological tissues used in the current study (T in degree K) [17–21]

Thermophysical property	Value	
Thermal conductivity, k (W/m K)	0.5	$273 < T$
	$15.98 - 0.0567 \times T$ $1005 \times T^{-1.15}$	$251 < T < 273$ $T < 251$
Volumetric specific heat, C (kJ/m ³ K)	3600	$273 < T$
	15,440 $3.98 \times T$	$251 < T < 273$ $T < 251$
Latent heat, L (MJ/m ³)	300	
Blood perfusion heating effect, $w_b C_b$ (kW/m ³ K)	40	

published examining the validity and mathematical consistency of the classical bioheat equation, and suggesting various alternatives [12,13]. Here, however, it is assumed that a more advanced model of bioheat transfer will not result in higher accuracy of the cryosurgery simulation. Furthermore, because such models involve greater mathematical complication, they were deemed unnecessary in this study. Note also that metabolic heat generation is typically negligible compared to the heating effect of blood perfusion and is therefore neglected in this study [14].

The scheme used here to solve Eq. (1) is based on a finite difference formulation:

$$T_{i,j,k}^{p+1} = \frac{\Delta t}{\Delta V_{i,j,k} [C_{i,j,k} + (\dot{w}_b C_b)_{i,j,k} \Delta t]} \sum_{l,m,n} \frac{T_{l,m,n}^p - T_{i,j,k}^p}{R_{l,m,n-i,j,k}} + \frac{\Delta t [(\dot{w}_b C_b)_{i,j,k} T_b + (\dot{q}_{met})_{i,j,k}] + C_{i,j,k} T_{i,j,k}^p}{C_{i,j,k} + (\dot{w}_b C_b)_{i,j,k} \Delta t} \quad (2)$$

where i, j, k and l, m, n are space indices, p is a time index, ΔV is an element unit volume, Δt is a time interval, and R is the thermal resistance to heat transfer between node i, j, k and its neighbor l, m, n . The numerical scheme described in Eq. (2) is conditionally stable, and a discussion regarding its applicability for cryosurgery has been presented by Rabin and Shitzer [9].

Table I lists typical values of the thermophysical properties of biological tissues, which were used in this study. Recently, Rabin [15] has studied how uncertainties in these thermophysical properties propagate through bioheat transfer simulations.

CRYOSURGERY PLANNING

The planning technique presented in this paper is general, and can be adapted to 3D problems. For the purposes of the current paper, however, we demonstrate our algorithm in 2D, on target regions typical of prostate cross sections.

Our technique does employ the notion of an objective function, however, it is not used in the traditional way. Our objective function is a measure of the total defect area, where defects are regions in the target area that have not been cryoinjured, and regions in the surrounding healthy tissues that have been. Rather than using the numerical value of the objective function to directly drive the optimization, we employ a force-field analogy based on the individual defect regions. The defects apply forces to the cryoprobes, tending to move them to locations that would reduce the value of the objective function. For our method, there is no need to compute gradients of the objective function.

Our objective function also serves a second role, which is determining the best outcome possible for a given configuration of cryoprobes. Once a configuration is selected, it is necessary to determine how long to run the procedure, i.e. how long the cryoprobes should be activated. If the cryoprobes are not operated long enough, some portions of the target region that could have been treated will not be. Conversely, if the cryoprobes are operated too long, healthy surrounding tissue will become cryoinjured. To determine the correct operating time, our software continually monitors the value of the objective function while computing the bioheat transfer simulation. When the value of the objective function reaches its minimum, the simulation is terminated. The time of termination is the optimal procedure time for that particular configuration of cryoprobes, however, that configuration may not be the optimal configuration.

An ideal configuration of cryoprobes would result in no defects. However, for the typical numbers of cryoprobes used in practice (typically between 5 and 12), the ideal solution is generally not achievable. Our approach searches for the minimum area of defects achievable for a specified number of probes, chosen by the cryosurgeon.

The Objective Function

In general the choice of objective function (the quantity to be minimized), dictates the quality of the solutions that can be found, and the speed with which they are obtained. The proposed objective function in this study, G , is the sum of all of the defect areas:

$$G = \int_A w dA \cong \sum_m w_m A_m \quad (3)$$

where A is the total area of the simulated problem, including both the target area and the surrounding tissue, w is a defect weighting function based on temperature, and m is an index representing all numerical grid points in the simulated 2D domain.

To evaluate the objective function, it is necessary to first define the temperature ranges that constitute defects in the solution. For example, one may wish to have all of the tissue in the target region be below -45°C , which is the commonly accepted to be the lethal temperature, i.e. a temperature threshold below which maximal cryoinjury is achieved [16]. One may further wish all of the tissue

outside the target region to be above 0°C, which is the lowest temperature before the destructive effect of ice crystallization is initiated. However, due to the physics of freezing, it is not possible to have such a step change in temperature at the boundary of the target region. Thus, even the best possible solution would have a significant defect area consisting of the tissue between the 0 and -45°C isotherms. The size of this transition region is dictated, to a large extent, by the thermophysical properties of the tissue. Thus, it cannot be completely eliminated by selecting better cryoprobe locations.

A clinical approach to this problem may be to match either the 0°C or the -45°C isotherm with the contour of the target region, creating the so-called “safety margins” interior or exterior to the target region, respectively. An alternative approach would be to allow the planning algorithm to split the area of the transition region between the target area and the healthy surrounding tissues. In the studies presented here, the -22°C isotherm was chosen as the temperature isotherm for optimization, which results in an almost exact split of the defect area between the target region and the surrounding healthy tissues. It is emphasized that any temperature isotherm could be used instead with our software. Ultimately, it will be up to the clinician to decide whether the safety margins should be interior to the target region, exterior to the target region, or distributed between the interior and exterior regions. It is noted that phase transition in biological tissues prevails over a wide temperature range, where -22°C is the lower boundary, assuming body solutions are closely approximated as an NaCl solution. It is further noted that phase transition may be affected by many factors such as biosolution concentrations and cooling rates. However, the current paper focuses on the planning algorithm, and one can replace the numerical scheme presented in Eq. (2) with any alternative scheme without affecting the planning algorithm. Nevertheless, the numerical technique presented above has been used intensively in the study of cryosurgery by this research team, as well as others. Accordingly, the defect weighting function is defined as follows:

$$w_m = \begin{cases} 1 & -22^\circ\text{C} < T_m & \text{interior to the target area} \\ 0 & T_m < -22^\circ\text{C} & \text{interior to the target area} \\ 1 & T_m < -22^\circ\text{C} & \text{exterior to the target area} \\ 0 & -22^\circ\text{C} < T_m & \text{exterior to the target area} \end{cases} \quad (4)$$

where T_m is the temperature at grid point m .

G (Eq. (3)) is the objective function to be minimized, but it also serves as the criterion for terminating the bioheat transfer simulation of the cryoprocure. As described above, the value of G is monitored during the simulation to determine the minimum value achievable for that configuration of cryoprobes. At the beginning of any simulation, the entire target region would be at normal body temperature, and thus the value of G would equal the area of the target region. In the early

stages of freezing, the interior defect area would decrease with time, as would the value of G . At a more advanced stage, freezing would begin to extend beyond the boundaries of the target region, and exterior defect regions would start to form. When the rate of growth of the exterior defect regions matches the rate of decrease of the interior defect regions, the total volume of defects would be at its minimum value. At this point, the cryosurgery simulation is terminated, and G has the smallest value possible *for that configuration* of the cryoprobes. Note, that this may not be the minimum value of the objective function, as other configurations may produce smaller values.

Force-field Analogy

The primary issue for our optimization technique is determining how to move the cryoprobes so as to achieve smaller values of the objective function. Rather than computing partial derivatives of the objective function with respect to the coordinates of the cryoprobes (or using other traditional optimization techniques), we use the defects in the temperature field to directly drive the improved cryoprobe locations. For this purpose, we introduce the concept of a force-field. The total force applied by the temperature field to a cryoprobe is given by:

$$\vec{F}_{nT} = \sum_m \frac{C_1}{|\vec{r}_{mn}|^2} w_m A_m \Delta T_m \vec{u}_{mn} \quad (5)$$

where \vec{F}_{nT} is the net force vector applied to cryoprobe n by all of the defects, C_1 is a constant, w_m is the weight function in Eq. (4), A_m is the cross sectional area associated with grid point m , \vec{r}_{mn} is a vector from grid point m to cryoprobe n , and \vec{u}_{mn} is a normalized version of \vec{r}_{mn} . ΔT_m is the difference between the temperature threshold for optimization and the temperature at grid point m , i.e. $\Delta T_m = (-22^\circ\text{C}) - T_m$. For external defects ΔT_m is positive, while for internal defects it is negative. Thus, the sign of ΔT_m indicates a repulsive force for external defects, and an attractive force for internal defects. The force applied by each defect is inversely proportional to the square of the distance from the defect to the cryoprobe. Thus the force falls off rapidly with distance, so that defects near a cryoprobe apply larger forces than those farther away. The rationale is that the cryoprobes nearest a defect are likely to have the largest influence on that defect. The force applied by a defect is also proportional to temperature difference, ΔT_m . This allows defect areas with more significant temperature differences (i.e. more significant defects) to apply larger forces, thus accelerating the optimization process.

Figure 1 shows a simple example of the force-field analogy. The temperature field shown is the result of multiple cryoprobes, however, for clarity only one is shown. To compute the force on the cryoprobe, Eq. (5) would be applied to each grid cell. However, for clarity, rather than showing the force that would be applied by

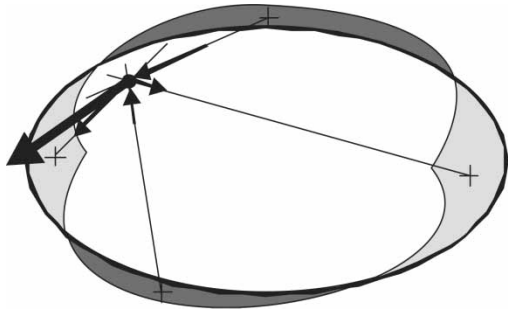


FIGURE 1 Illustration of the forces acting on a cryoprobe. Thick oval is boundary of target region. Dark shaded regions are exterior defect areas (cryoinjured healthy tissue). Light shaded regions are interior defect areas (uninjured target tissue). A plus sign (“+”) indicates the centroid of a defect area. Small arrows are forces applied by individual defect areas. The large arrow is the net force on the cryoprobe.

each cell, the figure shows the resultant of those forces for each of the four contiguous defect areas. Note that the resultant force applied by such an area would act through the area’s centroid, which is shown with a plus sign (“+”). Although there are four distinct, contiguous defects, only two of them apply significant forces to the cryoprobe shown in the figure: this cryoprobe is closest to the defects at the top and at the left of the figure, thus they apply the largest forces to the cryoprobe. Moving the cryoprobe in the direction of the resultant of all of the forces would tend to eliminate these two defects. (Moving the other cryoprobes not shown, would tend to eliminate the other defects.)

In order to prevent congestion of many cryoprobes at the same location, a short acting repulsive force is applied between cryoprobes:

$$\vec{F}_{nP} = \sum_j \frac{C_2}{|\vec{r}_{jn}|^3} \vec{u}_{jn} \quad (6)$$

where \vec{F}_{nP} is the net force vector applied to cryoprobe n by all of the other cryoprobes, j is the cryoprobe index, C_2 is a constant, \vec{r}_{jn} is a vector from cryoprobe j to cryoprobe n , and \vec{u}_{jn} is a normalized version of \vec{r}_{jn} . This force is inversely proportional to the cube of the distance between cryoprobes so that the force is negligible unless the cryoprobes are very near one another.

Moving Cryoprobes

When a cryoprobe is selected to be moved by our planning algorithm, it is moved in proportion to the net force it experiences:

$$\Delta\vec{r}_n = C_0(\vec{F}_{nT} + \vec{F}_{nP}) \quad (7)$$

where $\Delta\vec{r}_n$ is the displacement and C_0 is a constant. Examining Eqs. (5)–(7) indicates that there are a total of three constants that influence this displacement: C_0 , C_1 , and C_2 . However, the constants appear only in products, and thus there are only two quantities that matter: $C_{01} = C_0C_1$ and $C_{02} = C_0C_2$. The values we use for these quantities are

2×10^{-11} and 1.2×10^{-10} , respectively. We obtained these values empirically, and have found them to work well in practice. Using larger values would result in larger displacements of the cryoprobes, which could accelerate the solution, but may cause the optimizer to overshoot the optimum configuration and terminate prematurely. Using smaller values would have the opposite effect.

To be consistent with the grid representation used for computing the bioheat transfer simulations, before the cryoprobes are displaced, $\Delta\vec{r}_n$ must be rounded to the nearest grid cell location. Furthermore, to prevent overshooting the optimum, we limit the maximum displacement to be three grid cells in the x and y directions. This is a conservative choice that was obtained empirically and has proven to work well. Clinical constraints also govern the cryoprobe displacements. For example, in the current study: cryoprobes are not permitted to be displaced outside the target region, they are not permitted to be placed in the urethra during prostate cryosurgery, and they are not permitted to be closer than 2 mm to the boundaries of the target region.

It is possible to move multiple cryoprobes on each iteration of optimization as a means of accelerating the solution process. However, if too many are moved simultaneously, we suspect that the optimizer could miss the optimum and terminate prematurely. Our approach is to move multiple cryoprobes when the defect area is large, and to move them one at a time otherwise. If the total defect area is less than 1/8 of the area of the target region, only the cryoprobe with the largest force (i.e. the largest value of $\Delta\vec{r}_n$) is moved. If the total defect area is larger than this, the three cryoprobes with the largest forces are moved. This scheme is based on empirical observations of our system. We have found this scheme to work well, however, it may be possible to move cryoprobes more aggressively without encountering convergence problems.

Planning Strategy

To begin the optimization process, it is necessary to select an initial configuration for the cryoprobes. For example, they can be randomly distributed within the target region, or the user can manually select a preferred initial configuration, based on his or her own clinical experience. (Several methods that we used in various computerized experiments are described in the “Results and Discussion” section.) Next, a bioheat transfer simulation is computed until the optimal termination time is reached. Then the forces on the cryoprobes are computed and one or more cryoprobes are moved accordingly. This provides the configuration for the next iteration. Ordinarily, the process repeats in this fashion for many iterations.

Eventually, an iteration will result in an increase, rather than a decrease, in the total defect area. This typically occurs when the configuration is nearly optimal, and the particular cryoprobe moved was already at an (locally) optimal location. Because this occurs when the solution is nearly optimal, the iteration typically involves moving just

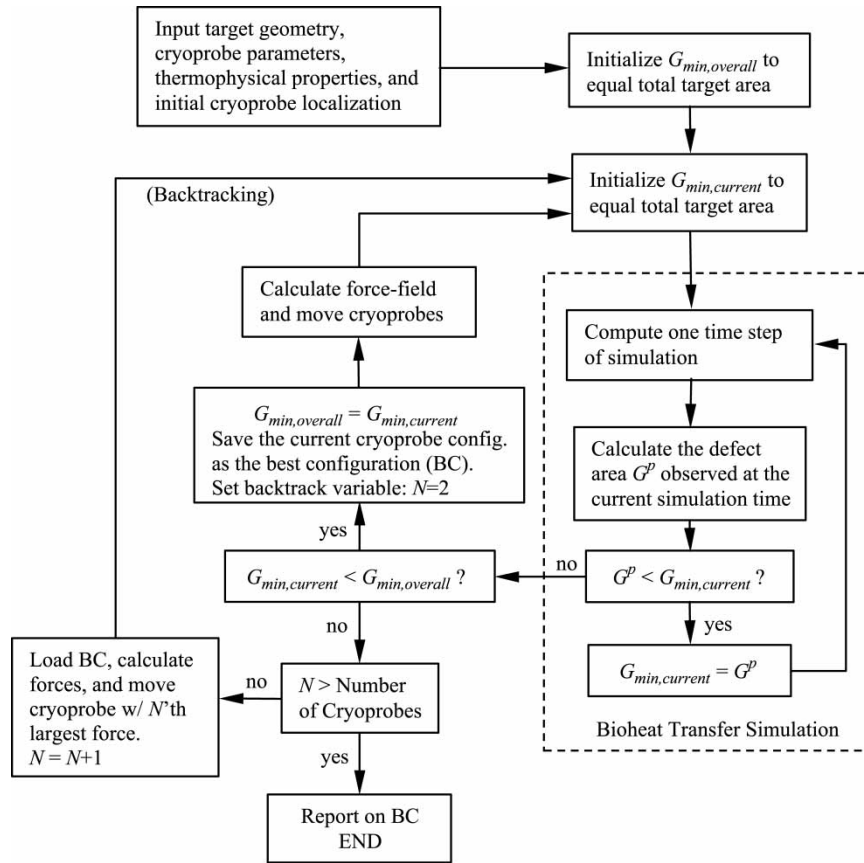


FIGURE 2 Planning algorithm: G^p is the objective function presented in Eq. (3), evaluated at time level p of the bioheat transfer simulation; $G_{min,current}$ is the minimum value calculated up to time level p for the current configuration of cryoprobes; $G_{min,overall}$ is the minimum value of $G_{min,current}$ from all configurations tested up to the current iteration of planning; N is a cryoprobe index in the backtracking process.

one cryoprobe. When this happens, the program begins a backtracking procedure. The iteration is rejected, and the cryoprobe that had the second largest force in the previous iteration is moved. If this again results in an increase in the defect area, the program again backtracks, this time moving the cryoprobe with the third largest force. Backtracking continues until either an improvement is achieved or the program backtracks through all of the cryoprobes. In the former case, the program continues on in the usual way. In the latter case, a local optimum has been found and the program terminates. The complete planning algorithm is shown in the flow chart in Fig. 2.

RESULTS AND DISCUSSION

For the purposes of the current report, the planning algorithm was demonstrated in 2D, on a cross sectional area typical of a prostate, shown in Fig. 3. For this study, the following parameters were used:

(1) The cryoprobe temperature was idealized by assuming a step like temperature change at the beginning of the process, dropping from 37 to -145°C , where -145°C is a typical operation temperature of Joule–Thomson cryoprobes working on Argon gas.

- (2) The cryoprobes had an external diameter or of 1 mm.
- (3) The diameter of the urethra was 6 mm. Consistent with current clinical applications of urethral warmers, the urethra was maintained at a temperature of 37°C throughout the cryogenic operation [17,18].
- (4) The prostate radius was 23 mm, which is consistent with a spherical volume of 50 ml. The prostate of a typical candidate for cryosurgery is in the range of 25–50 ml.
- (5) The simulated cross sectional area, including the prostate and surrounding healthy tissues, was $120\text{ mm} \times 120\text{ mm}$. Because of symmetry, only one half of this cross section was considered. A zero heat flux thermal boundary condition was used for the outer perimeter of the cross section. For the duration of the simulated procedure, the temperature at the outer boundary was found to be unchanged from its initial temperature, indicating that the domain could be considered infinite from the perspective of heat transfer.
- (6) For computing bioheat transfer simulations, a $1\text{ mm} \times 1\text{ mm}$ mesh was used.
- (7) The values used for the thermophysical properties are as listed in Table I.
- (8) For the purposes of accurately identifying the defect regions, the numerical grid used to compute

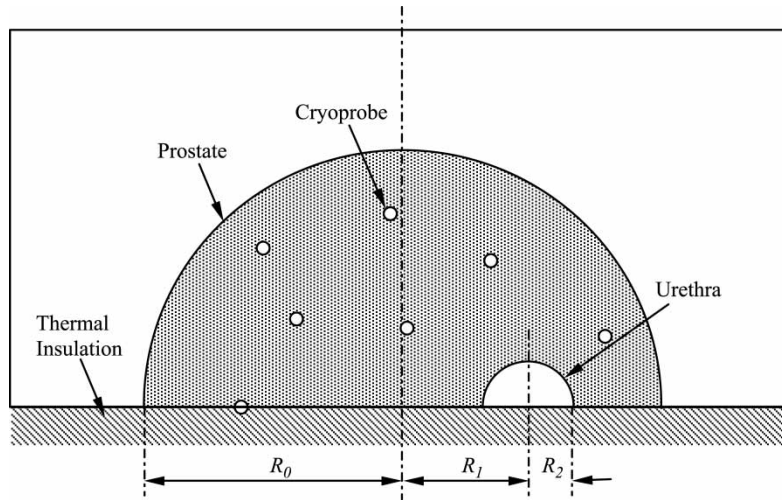


FIGURE 3 Schematic illustration of the prostate cross section. Because of symmetry, only half of the cross section was considered in the bioheat transfer simulation.

the bioheat transfer simulations was interpolated. Each $1\text{ mm} \times 1\text{ mm}$ grid cell was divided into 100 sub-cells, each $0.1\text{ mm} \times 0.1\text{ mm}$. The temperatures on this finer grid were interpolated from the values on the larger grid using bilinear interpolation. In this paper, index m in Eqs. (3)–(7) refers to this finer grid.

- (9) For each experiment, the number of the cryoprobes was fixed throughout the entire planning process. Various experiments used between 4 and 14 cryoprobes.

To evaluate the planning algorithm, two general cases were studied. The first is a circular prostate cross section with the urethra located at the center. The second is also a circular cross section, however, the urethra is off center by

8 mm ($R_1 = 8\text{ mm}$ in Fig. 3), thus providing a more anatomically realistic problem.

To test the robustness of the planning algorithm, various initial configurations of cryoprobes were explored as shown in Fig. 4. For the centered urethra case, the initial configuration was a circle with a radius equal to half that of the cross section (configuration A). For the offset urethra case, the circular distribution was also used: configuration B is a circular distribution with two cryoprobes on the symmetry line, while configuration C has no cryoprobes on the symmetry line. Configuration D is a random distribution of cryoprobes, while configuration E is a linear distribution, with all cryoprobes in a vertical line on one side of the cross section. Configurations A–C were intended to be examples of

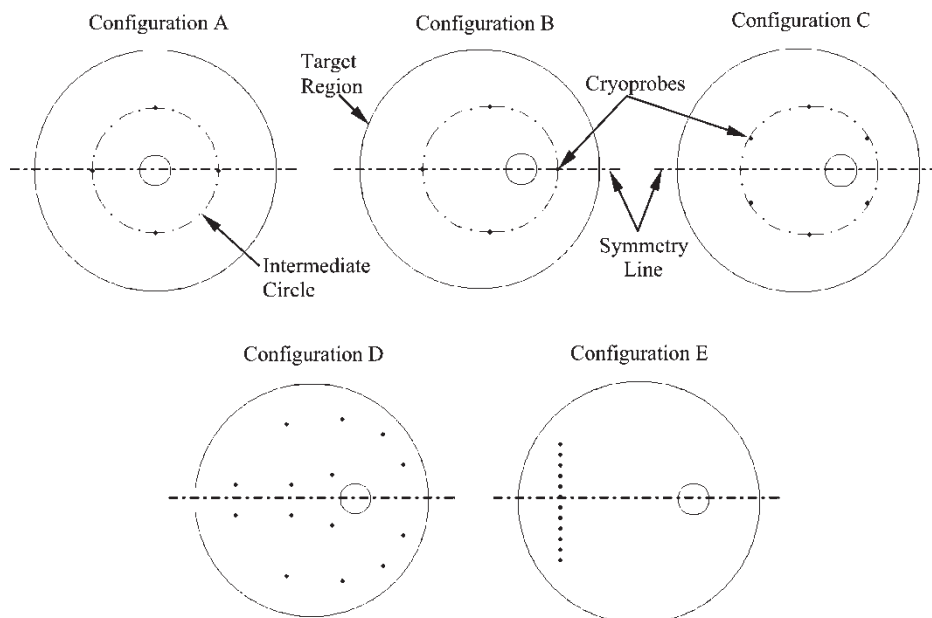


FIGURE 4 Schematic illustration of initial configurations tested in this study. In configuration A the urethra is centered, while it is off center in configurations B–E: (A) intermediate circle, (B) intermediate circle with two cryoprobes on the symmetry line, (C) intermediate circle with no cryoprobes on the symmetry line, (D) random configuration, and (E) stacked configuration.

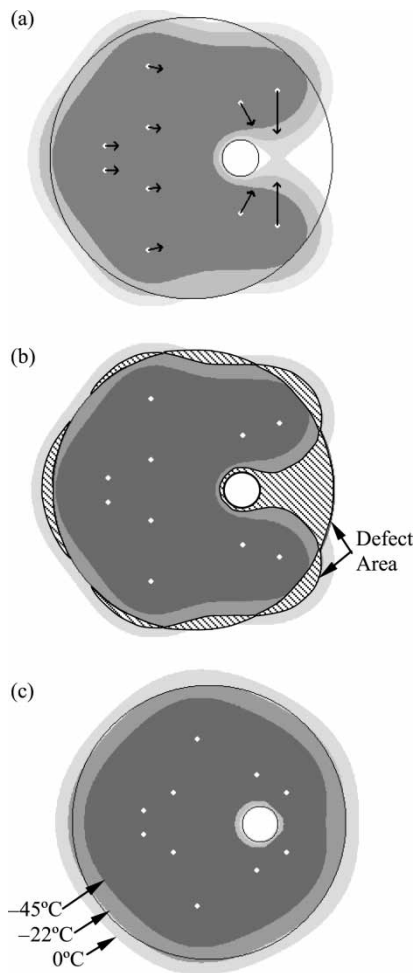


FIGURE 5 Planning starting from a random initial configuration (case D in Fig. 4). Cryoprobes are represented as white circles. (a) The temperature regions and forces on cryoprobes at the end of simulation for the initial configuration. (b) Defects at the end of simulation for the initial configuration. (c) The temperature regions at the end of simulation for the optimal configuration.

good initial configurations, while D and E were intended to be bad examples.

Figure 5 shows a typical problem, with 10 cryoprobes and a random initial configuration (configuration D in Fig. 4). Figure 5a shows the temperature field when the total defect area reaches a minimum for the initial configuration, and the resulting forces that would be applied to the cryoprobes. Figure 5b shows the defects at the end of the bioheat transfer simulation of the initial configuration. Notice that the forces do indeed tend to move the cryoprobes so as to eliminate defects. For example, the cryoprobes nearest the internal defect on the right side of the cross section are strongly pulled towards that defect. Figure 5c shows the optimal solution, which took a total of 18 iterations (including backtracking).

The results of all of the experiments are listed in Table II. The experiments demonstrated that the quality of the final solution is insensitive to the initial configuration, however, the amount of work required to obtain the optimum does depend on it. Regardless of the initial

configuration, the total defect area was less than 5% for a planned procedure with at least 6 cryoprobes.

For circular initial configurations an average of about 13 iterations were needed, for random configurations about 24, and for linear about 70. In general, the circular distribution appears to be a good initial configuration for prostate problems. Surprisingly, even a random distribution makes a reasonable starting point, most likely because such configurations tend to distribute the cryoprobes uniformly throughout the target area. In fact, for procedures in which the target area is irregular, a random distribution may be a convenient starting point.

While the total defect area is relatively insensitive to the number of cryoprobes used, the expected time of the cryoprocure depends on it strongly (right column in Table II). For example, with only 4 cryoprobes, the freezing would require more than a half hour, which is unrealistically long for a surgical procedure. For 6 cryoprobes, only 9–14 min would be required; for 8 or more, less than 9 min would be required, which is clinically realistic. Our current objective function considers only the total defect area, and not the procedure duration. Thus, the solutions generated may not be time optimal. For example, with 6 cryoprobes and random initial configuration, one of the plans in Table II requires only 8.6 min of freezing while another requires 14.2, although they have nearly identical total defect areas. Based on this observation, it would be useful to modify our objective function so as to minimize freezing duration in addition to defect area.

As described above in the “Planning Strategy” section, the final stages of planning involve a sequence of backtracking steps. When the configuration is (locally) optimal, moving a cryoprobe results in an increase in the net defect area, thus necessitating that the move be rejected. The planning terminates when the program has backtracked through all of the cryoprobes and has determined that no further improvement can be achieved. The total amount of computation required for backtracking is proportional to the number of cryoprobes. However, the run time of each bioheat transfer simulation is inversely proportional to the number of cryoprobes because with larger numbers of cryoprobes, the freezing is faster. Thus, the two effects offset one another. Nevertheless, if program execution time is critical, the program could be terminated earlier, when the total defect area reaches a threshold of perhaps 4 or 5%.

As can be seen in Table II, for circular initial configurations (cases A–C), the number of planning iterations is typically between one and two times the number of cryoprobes. For random initial configurations (case D), the number of iterations is about triple the number of cryoprobes. Thus, if there are n cryoprobes, the number of bioheat transfer simulations that would be required is between n and $3n$. It is interesting to compare this to the number that would be required with a conventional optimization technique, such as gradient descent or sequential quadratic programming [3]. For each

TABLE II Case study of the effect of the initial configuration of cryoprobes on planning results. See Fig. 4 for definitions of initial configurations A–E. Problems with random initial configurations (D) were repeated at least once

Number of cryoprobes	Initial configuration	Number of iterations required	Total interior defect area (mm ²)	Total exterior defect area (mm ²)	Total defect area in comparison with the target area (%)	Simulated time (min)
4	A	12	67.3	4.6	4.4	35.8
6	A	5	19.5	26.8	2.8	8.8
8	A	9	19.2	14.9	2.1	6.3
10	A	13	8.9	17.5	1.6	5.6
12	A	11	8.1	16.4	1.5	4.8
14	A	11	14.6	15.0	1.8	4.5
4	B	6	50.2	23.3	4.5	34.5
6	B	10	25.8	14.7	2.5	13.3
8	B	13	10.5	18.5	1.8	8.7
10	B	13	8.4	18.5	1.7	6.6
12	B	21	12.5	27.1	2.4	4.5
14	B	27	15.7	13.3	1.8	4.7
4	C	3	67.0	20.6	5.4	31.1
6	C	10	16.6	30.8	2.9	12.2
8	C	11	9.0	18.9	1.7	8.0
10	C	14	10.8	20.8	1.9	6.2
12	C	17	16.3	22.3	2.4	5.0
14	C	34	8.4	20.4	1.8	4.3
6	D	8	41.5	36.8	4.8	8.6
6	D	17	35.0	40.8	4.6	14.2
8	D	13	26.6	35.4	3.8	7.1
8	D	25	17.8	18.3	2.2	8.9
10*	D	18	22.0	42.1	3.9	5.4
10	D	24	26.5	28.4	3.4	4.8
10	D	29	24.6	39.9	4.0	4.8
12	D	40	10.9	40.2	3.1	3.7
12	D	28	21.4	20.1	2.5	3.0
14	D	29	13.7	27.1	2.5	2.6
14	D	29	12.4	38.8	3.1	2.6
5	E	58	64.9	42.9	6.6	26.6
8	E	54	18.7	28.4	2.9	13.3
11	E	76	26.2	26.5	3.2	4.6
14	E	89	20.7	26.1	2.8	3.7

* Presented in Fig. 5.

iteration with such techniques, it would be necessary to compute the partial derivatives of the objective function, Eq. (3), with respect to the x and y coordinates of each cryoprobe. Each partial derivative would require one bioheat transfer simulation in which a cryoprobe is displaced a small amount in either x or y , for a total of $2n$ bioheat transfer simulations per iteration. Thus the number of simulations required for each iteration is comparable to the total number required with our force-field approach. If only 10 iterations were required with the convention approaches (a very conservative estimate), our approach would be an order of magnitude more efficient.

Our planning algorithm is similar to hill climbing search, which always converges to a local optimum (assuming there is one) [22]. In hill climbing, one parameter is changed at a time, and it is changed to the next nearest value. By analogy, our optimizer would be guaranteed to converge to a local optimum if a single cryoprobe was moved on each step, and that cryoprobe was moved just one grid space. However, operating in this fashion would increase computation time unnecessarily. Instead, we move cryoprobes in proportion to the force magnitudes and sometimes move multiple cryoprobes simultaneously. In our experiments, we have found that we get rapid convergence to high quality solutions.

As with most numerical optimization techniques, our optimizer terminates at the first optimum found. Often this is a local rather than the global optimum. Furthermore, the particular optimum found depends on the initial configuration of the cryoprobes. This is why the results in Table II indicate small variations in the total defect area for different initial conditions.

The results presented here were obtained on a Pentium 4 computer, with a 2.4 GHz processor, a 533 MHz front side bus, and 256 MB of PC2700 DDR memory. The software was implemented with Visual Studio 6.0 and executed under Windows XP Professional. Although our planning technique has proven to be efficient, typical planning times ranged from 1.5 to 4 h per problem, which is still too long for clinical applications. The longest execution times occurred when there were only 4 cryoprobes, because with so few cryoprobes, the freezing process, and thus the simulation, is slow. Although most of the execution time was due to simulation, there may be ways to further increase the efficiency of our force-field optimization technique. For example, it is likely that we can increase efficiency by increasing the number of cryoprobes moved on a single iteration and by increasing the distance by which they are moved (i.e. finding better values for C_{01} and C_{02}). Additionally, we may be able to reduce computation by

developing techniques for finding better initial configurations. We are addressing these issues in ongoing work.

However, because most of the computational cost is due to computing simulations, the most effective way to reduce execution time is to develop faster simulation techniques. The 2D examples explored here were intended to demonstrate the feasibility and efficiency of our force-field approach. However, to provide a planning tool useful for clinical applications, we are extending our approach to 3D. This increases the cost of simulation by an order of magnitude, thus further necessitating the development of faster simulation techniques. We have begun work in this area, and our initial results are quite promising.

CONCLUSIONS

The purpose of the cryosurgery planning tool developed in this study is to identify the best locations for the cryoprobes so as to maximize the amount of the target region that is cryoinjured, while minimizing cryoinjury external to the target region. This is an optimization problem in which the objective function involves computing a bioheat transfer simulation of freezing. Such simulations are computationally expensive. To reduce computation time, a novel optimization technique was developed. The technique requires only one simulation per iteration of optimization, which is significantly more efficient than conventional optimization techniques, where conventional optimization techniques would typically require multiple simulations per iteration. The new technique is based on a force-field analogy, in which regions of tissue that would have undesirable temperatures apply forces to the cryoprobes, directly moving them to better locations.

The new technique has been used to create a prototype 2D planner. Experiments with the planner have demonstrated that the technique is at least an order of magnitude more efficient than traditional optimization techniques for this problem. Often only 10–20 iterations are needed to create an optimal plan. The experiments also demonstrated that a good final configuration could be found regardless of the quality of the initial configuration. For example, for procedures including at least 6 cryoprobes, the planner was always able to find solutions with a total defect area less than 5% of the target area. However, starting from a good initial configuration does allow the planner to find an optimal solution with fewer iterations.

Starting from different initial configurations, it is possible to obtain different solutions that all have about the same defect area. These solutions may differ, however, with regard to other parameters of interest to the cryosurgeon, such as the procedure duration. This suggests that it may be useful to augment the current objective function to consider other clinically important parameters in addition to defect area.

Although the planning technique has been demonstrated in 2D, it can be directly adapted to 3D problems. The main difficulty in moving to 3D is the higher cost of

computing bioheat transfer simulations. In ongoing work, we are developing more efficient simulation techniques to make 3D planning feasible.

Acknowledgements

This work is supported in part by the Pennsylvania Infrastructure Technology Alliance, a partnership of Carnegie Mellon, Lehigh University, and the Commonwealth of Pennsylvania's Department of Economic and Community Development.

References

- [1] Cooper, I.S. and Lee, A. (1961) "Cryostatic congelation: a system for producing a limited controlled region of cooling or freezing of biological tissues", *J. Nerv. Ment. Dis.* **133**, 259–263.
- [2] Chang, Z., Finkelstein, J.J., Ma, H. and Baust, J. (1994) "Development of a high-performance multiprobe cryosurgical device", *Biomed. Instrum. Technol.* **28**, 383–390.
- [3] Vanderplaats, G.N. (1984) *Numerical Optimization Techniques for Engineering Design* (McGraw-Hill, New York).
- [4] Keanini, F.G. and Rubinsky, B. (1992) "Optimization of multiprobe cryosurgery", *Trans. ASME* **114**, 796–801.
- [5] Kincaid, D. and Cheney, W. (1996) *Numerical Methods*, 2nd ed. (Brooks/Cole Publishing, Pacific Grove, CA).
- [6] Shimada, K. and Gossard, D. (1998) "Automatic triangular mesh generation of trimmed parametric surfaces for finite element analysis", *Comput. Aided Geometric Des.* **15**(3), 199–222.
- [7] Yamakawa, S., Shimada, K. (2000) High quality anisotropic tetrahedral mesh generation via packing ellipsoidal bubbles, *The 9th International Meshing Roundtable*, pp. 263–273.
- [8] Kim, J. (1989) Reasoning on the location of components for assembly Packing, in *Proc. of ASME Design Automation Conference*, Montreal.
- [9] Rabin, Y. and Shitzer, A. (1998) "Numerical solution of the multidimensional freezing problem during cryosurgery", *ASME J. Biomech. Eng.* **120**(1), 32–37.
- [10] Pennes, H.H. (1948) "Analysis of tissue and arterial blood temperatures in the resting human forearm", *J. Appl. Phys.* **1**, 93–122.
- [11] Rabin, Y., Coleman, R., Mordohovich, D., Ber, R. and Shitzer, A. (1996) "A new cryosurgical device for controlled freezing. Part II: *In vivo* experiments on rabbits' hind thighs", *Cryobiology* **33**, 93–105.
- [12] Charny, C.K. (1992) "Mathematical models of bioheat transfer", In: Hartnett, J.P., Irvine, T.F. and Cho, Y.I., eds, *Advances in Heat Transfer* (Academic Press, New York), pp 19–156.
- [13] Diller, K.R. (1992) "Modeling of bioheat transfer processes at high and low temperatures", In: Hartnett, J.P., Irvine, T.F. and Cho, Y.I., eds, *Advances in Heat Transfer* (Academic Press, New York), pp 157–358.
- [14] Eberhart, R.C. (1985) "Thermal models of single organs", In: Shitzer, A. and Eberhart, R.C., eds, *Heat Transfer in Biology and Medicine* (Plenum Press, New York), pp 261–324.
- [15] Rabin, Y. (2003) "A general model for the propagation of uncertainty in measurements into heat transfer simulations and its application to cryobiology", *Cryobiology* **46**(2), 109–120.
- [16] Gage, A.A. and Baust, J. (1998) "Mechanisms of tissue injury in cryosurgery", *Cryobiology* **37**(3), 171–186.
- [17] Rabin, Y. and Stahovich, T.F. (2002) "The thermal effect of urethral warming during cryosurgery", *CryoLetters* **23**, 361–374.
- [18] Rabin, Y. and Stahovich, T.F. (2003) "Cryoheater as a means of cryosurgery control", *Phys. Med. Biol.* **48**, 619–632.
- [19] Altman, P.L. and Dittmer, D.S. (1971) *Respiration and Circulation*. Federation of American Societies for Experimental Biology (Data Handbook, Bethesda, MD).
- [20] Chato, J.C. (1985) "Selected thermophysical properties of biological materials", In: Shitzer, A. and Eberhart, R.C., eds, *Heat Transfer in Biology and Medicine* (Plenum Press, New York), pp 413–418.
- [21] Rabin, Y. (2000) "The effect of temperature-dependent thermophysical properties in heat transfer simulations of biomaterials in cryogenic temperatures", *CryoLetters* **21**, 163–170.
- [22] Winston, P.H. (1992) *Artificial Intelligence*, 3rd ed. (Adison-Wesley Publishing, Reading, MA).